

2014

# Optimal Chiller and Thermal Energy Storage Design for Building HVAC Systems

David I. Mendoza-Serrano

*Illinois Institute of Technology, United States of America, dmendoz1@hawk.iit.edu*

Donald J. Chmielewski

*Illinois Institute of Technology, United States of America, chmielewski@iit.edu*

Follow this and additional works at: <http://docs.lib.purdue.edu/ihpbc>

---

Mendoza-Serrano, David I. and Chmielewski, Donald J., "Optimal Chiller and Thermal Energy Storage Design for Building HVAC Systems" (2014). *International High Performance Buildings Conference*. Paper 117.  
<http://docs.lib.purdue.edu/ihpbc/117>

This document has been made available through Purdue e-Pubs, a service of the Purdue University Libraries. Please contact [epubs@purdue.edu](mailto:epubs@purdue.edu) for additional information.

Complete proceedings may be acquired in print and on CD-ROM directly from the Ray W. Herrick Laboratories at <https://engineering.purdue.edu/Herrick/Events/orderlit.html>

## Optimal Chiller and Thermal Energy Storage Design for Building HVAC Systems

David I. MENDOZA-SERRANO, Donald J. CHMIELEWSKI\*

Illinois Institute of Technology, Department of Chemical Engineering,  
Chicago, IL, USA

Contact Information (Phone: 312.567.3537, Fax: 312.567.8874, chmielewski@iit.edu)

\* Corresponding Author

### ABSTRACT

In the context of indoor building temperature regulation, a controller calculates the inputs for the HVAC system that result in appropriate thermal comfort conditions. Additionally, if electricity prices are time dependent, these control actions will also impact economic expenditures. To improve economic performance, Thermal Energy Storage (TES) is typically used in conjunction with HVAC to time-shift chiller cooling loads to times of low energy price. The method of Economic Model Predictive Control (EMPC) has been demonstrated to effectively reduce expenditures. Since TES and chiller sizes have a direct impact on achievable operational savings, an economic analysis considering the investment costs associated with these equipments is necessary. This work presents a novel algorithm intended to optimally select equipment sizes based on Net Present Value analysis and utilizing the recently developed methods of Economic Linear Optimal Control (ELOC) and constrained ELOC. Implementation of the numeric optimization is illustrated with a case study.

### 1. BACKGROUND

Typical smart grid policies provide economic incentives as well as surcharges aimed to regulate electricity consumption (Farhangi, 2010; Ipakchi and Albuyeh, 2009). Common policies that exemplify this behavior are real time pricing (RTP) and Time of Use (TOU) scenarios (Walawalkar *et al.*, 2010). When electricity demand is dominant, prices tend to increase and when supply is abundant, to decrease. A direct effect of these methodologies on building thermal comfort regulation is that operating costs from HVAC equipment tend to be higher at the hottest times of a day. This is because in summertime weather conditions, electricity demand and electricity costs exhibit strong correlations (Ercot, 2012; NCDC, 2012). To de-correlate time of electricity consumption from weather conditions, Thermal Energy Storage (TES) can be utilized (Henze *et al.*, 2003). TES typically relies on a cooling media. Ice, chilled water and phase change materials (PCM) are common examples. The energy stored, using TES at times low electricity prices, can then be recovered when electricity prices are at their peak. However, this additional equipment has an associated investment, maintenance and operational costs (Chen *et al.*, 2009). Hence, the question that comes to mind is: “Does the reduction in expenditure offset the cost of additional hardware?” Consequently, adequate quantitative methods for equipment sizing and optimization are required. Despite this evident need, optimization based equipment sizing methods appear to be lacking in the literature, especially when compared to the wealth of propositions available for equipment control. Thus, this work is specifically devoted to the development of an algorithm to optimally select equipment sizes based on Net Present Value analysis and in the closed-loop context of Economic Model Predictive Control (EMPC).

#### 1.1 Case Study Description

Figure 1 (left) depicts the thermal interactions between a typical building, chiller and the active TES unit. The TES unit adds a degree of freedom by allowing for independent manipulation of heat flow to the chiller,  $Q_c$ , and heat flow from the room,  $Q_r$ . Energy in the TES unit,  $E_s$ , is the time integral of storage heat flow,  $Q_s$ . Figure 1 (right) depicts the basic building configuration to be used. The state space model is:  $\dot{s} = As + Bm + Gp$ ,  $q = D_x s + D_u m$ , where  $s$  is the state vector,  $m$  is the vector of manipulated variables,  $p$  is the disturbance and  $q$  indicates the point-

wise-in-time restrictions:  $q^{\min} \leq q(t) \leq q^{\max}$ , where  $s = [T_0 \ T_{11} \ T_{12} \ T_{21} \ E_s]^T$   $p = [T_3 \ C_e]^T$   $m = [Q_s \ Q_c]^T$   $q = [T_0 \ E_s \ Q_r \ Q_c]^T$   $q^{\max} = [T_0^{\max} \ E_s^{\max} \ Q_r^{\max} \ Q_c^{\max}]^T$  and  $q^{\min} = [T_0^{\min} \ E_s^{\min} \ Q_r^{\min} \ Q_c^{\min}]^T$ . Further details on the building model can be found in Mendoza-Serrano (2013) and Mendoza-Serrano and Chmielewski (2012a, 2012b and 2014).

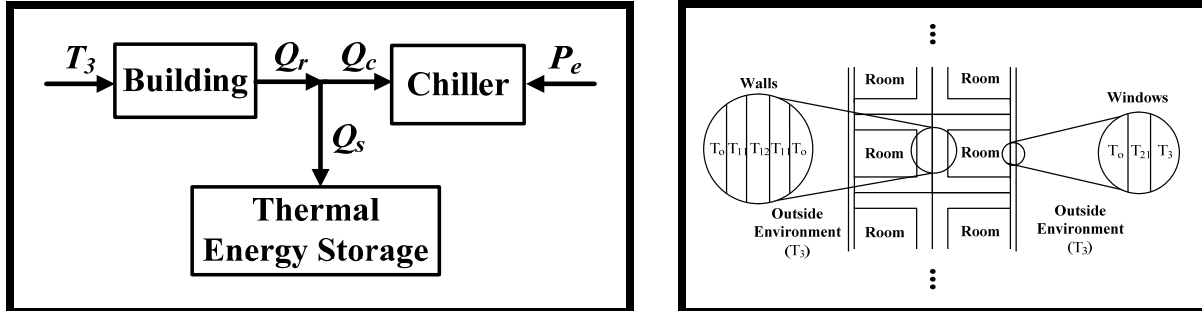


Figure 1: Left: Process diagram for HVAC system with TES. Right: Description of building zones

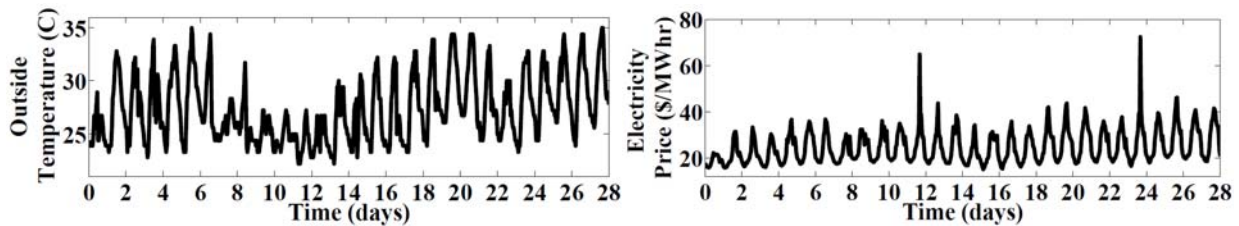


Figure 2: Outside temperature and electricity prices for July 2012 in Houston, TX (Ercot, 2012; NCDC, 2012)

## 1.2 Economic MPC for Building HVAC with TES

To implement a predictive type controller, the continuous-time model must be first converted to the following discrete-time predictive form (sample period  $\Delta t_s = 1$  hour). The time index  $i$  represents actual time and  $k$  is predictive time.

$$s_{k+1|i} = A_s s_{k|i} + B_s m_{k|i} + G_d p_{k|i} \quad (1)$$

$$q_{k|i} = D_x s_{k|i} + D_u m_{k|i} \quad (2)$$

$$q^{\min} \leq q_{k|i} \leq q^{\max} \quad (3)$$

The historic data of Figure 2 is used for the outside temperature,  $T_3$ , and electricity price,  $C_e$ . As expected the cost of electricity has a clear correlation with outside temperature, due to the increases in power demand during the hottest hours of a summer day. The cost of operating the chiller at time  $i$  is given by  $C_{e,i} P_{c,i} \Delta t_s$ , where  $P_{c,i}$  is the electric power to the chiller and  $P_{c,i} = \eta Q_{c,i}$ ,  $\eta = 0.3 MW_e / MW_T$ . Thus, the EMPC problem to be solved at each time  $i$  is:

$$\min_{s_{k|i}, m_{k|i}, q_{k|i}} \left\{ \frac{\Delta t_s \eta}{N} \sum_{k=i}^{i+N-1} C_{e,k|i} Q_{c,k|i} \right\} \quad s.t. \quad (1), (2), (3) \text{ and } s_{ij} = s_i \quad (4)$$

Then, given the solution to problem (4) the actual manipulation sent to the process is first value of the predicted manipulation:  $m_i = m_{ij}$ . Figure 3 illustrates the closed-loop implementation of EMPC with three TES size assumptions. In the case of no TES the cost of operation for the 28 days is \$759. If given a storage unit with a capacity of  $3.0 MW_{7hr}$ , the operating cost is reduced by 39% to \$464. If the capacity is  $1.5 MW_{7hr}$ , then the operating cost is \$521, a reduction of only 31%. The left plot of Figure 3 clearly illustrates the time-shift in that heat to the chiller (proportional to power consumption) is greatest when outside temperature and electricity prices are low. The controller of the right plot attempts to do the same, but is frustrated by the smaller size of the TES. Specifically, when the storage limits are encountered the chiller must go back to operation similar to the no TES case. It is finally noted that there appears to be a nonlinear relationship between TES size and operating cost savings.

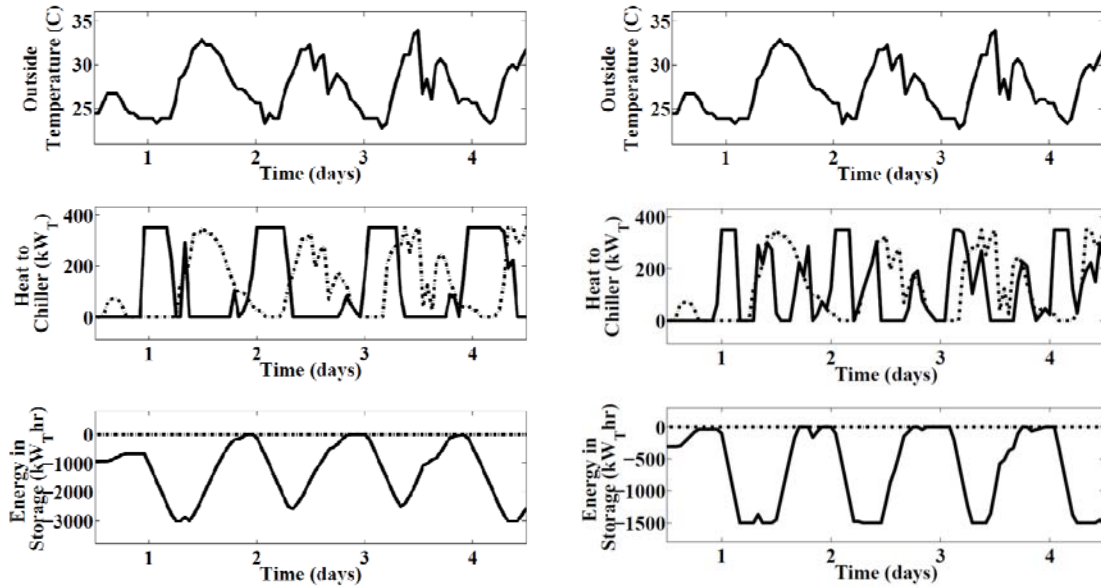


**Figure 3:** Closed-loop EMPC simulations. Dashed – no TES, Solid left –  $3.0MW_7hr$  of TES, Solid right –  $1.5MW_7hr$  of TES. All with an EMPC prediction horizon of 24hrs

### 1.3 Equipment Sizing Framework and Challenges

The goal of the sizing algorithm is to maximize net present value

$$NPV = - PV_f \bar{R} - CapCosts \quad (5)$$

In this work, we assume the capital cost of a chiller, with maximum power capacity of  $P_c^{max}$ , is  $c_c P_c^{max}$ . Similarly, the purchase cost of a TES unit with maximum storage capacity of  $E_s^{min}$ , is assumed to be  $c_s E_s^{min}$  (where  $c_s < 0$  due to the sign convention of  $E_s^{min} < 0$ ). As in earlier sections, the instantaneous expenditure (in  $\$/hr$ ) is given by  $R = C_e P_c$ . Thus, the average expenditure (also in  $\$/hr$ ) is

$$\bar{R} = E[C_e P_c] \approx \frac{1}{M} \sum_{i=0}^M C_{e,i} P_{c,i} \quad (6)$$

where  $M$  is the total number of periods in the evaluation. For example, if the evaluation is over one month, then  $M = 24 \times 28$ . It is also noted that  $C_{e,i}$  and  $P_{c,i}$  are the actual or realization values of the evaluation, which are different than the predicted values of (4) used to solve the EMPC problem. Finally, the present value factor is defined as (where  $r_i$  is the annual interest rate and  $n$  is the project horizon in years):

$$PV_f = 365 \times 24 \frac{1}{r_i} \left[ 1 - \frac{1}{(1+r_i)^n} \right] \quad (7)$$

One approach to the equipment sizing problem is to run several EMPC simulations with various equipment sizes and manually select those with the largest  $NPV$ . Similarly, one could use the EMPC simulations within a simple gradient search algorithm (see Figure 4, left). Specifically, a simulation will be run using EMPC in closed-loop and based on the chiller and TES sizes provided by the gradient search block. The resulting evaluation of average expenditure is then sent to the gradient search algorithm, which decides on a new set of equipment sizes to evaluate until no more improvements to  $NPV$  can be found.

Despite the intuitive nature of this approach, several issues are clearly evident. The first issue is the selection of initial point for the gradient search. The second is issue is the lack of a guarantee of global optimality for such an algorithm. The third concerns the scenario of a postulated equipment size being such that cooling needs of the building cannot be satisfied (or EMPC is not successful in satisfying those needs). Finally, there is the concern of each EMPC based evaluation of average expenditure requiring too much computational effort. To the last point it is noted that computation time of the 28 day simulations of the previous sub-section took approximately 1.4 hours

each. One approach to reduce computational effort is to reduce the EMPC prediction horizon. For example, changing the horizon from 24 hrs to 3 hrs, will bring the 28 day simulation time down to just 6.7 seconds. However, much of the operating cost savings will be lost (for the 1.5 MW<sub>thr</sub> case the savings drops from 31% to only 14%). This lack of performance is denoted as inventory creep (Lima *et al.*, 2011) as illustrated in the right plot of Figure 4. Specifically, the short horizon of EMPC causes it to use up all stored energy for short term gain as it is not aware of the value of storing energy for future use. It thinks there is no future beyond its prediction horizon. Mitigation (or avoidance) of these issues will be facilitated by the newly developed method of Economic Linear Optimal Control (ELOC) described next.

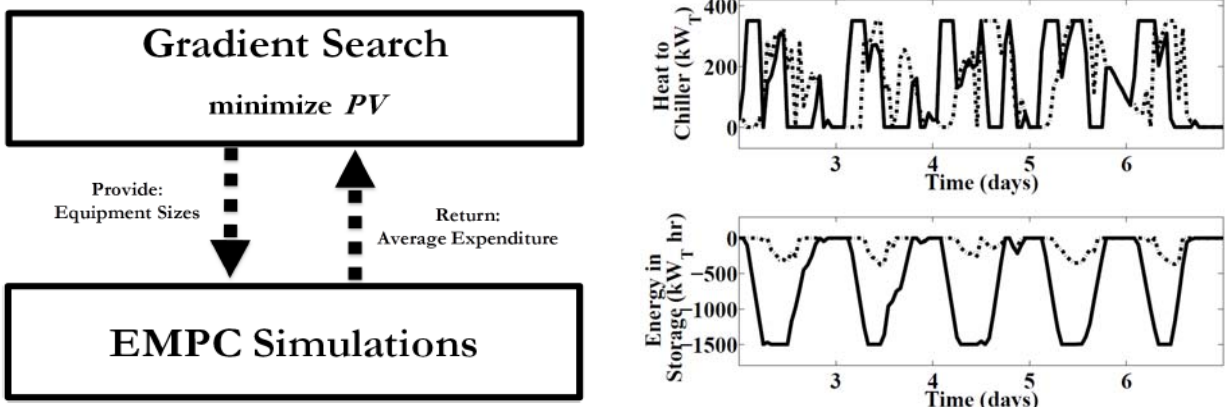


**Figure 4:** Left – Illustration of the gradient search algorithm. Right – Illustration of inventory creep.

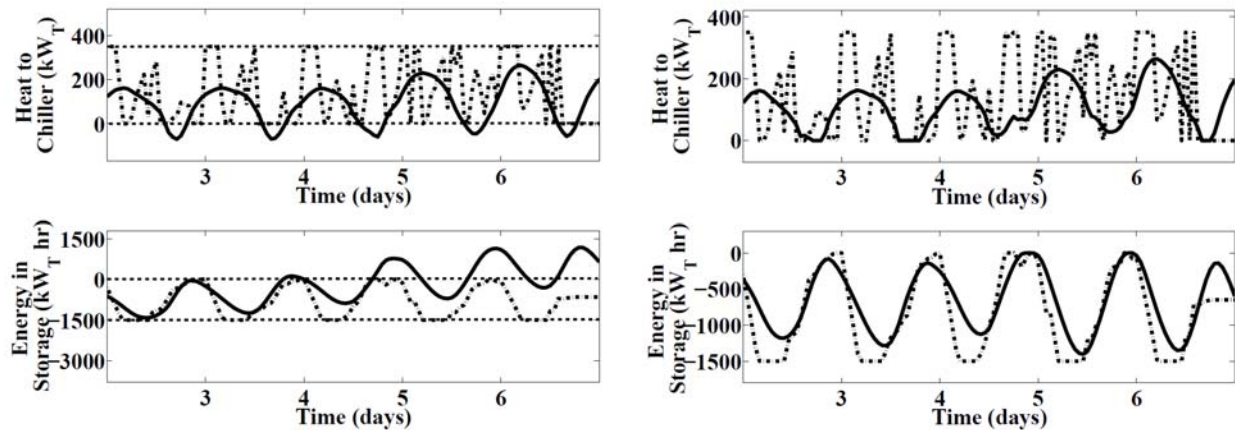


**Figure 5:** Left – Application of ELOC (solid) and EMPC (dashed) policies. Right – Application of Constrained ELOC (solid) and EMPC (dashed) policies, both with a 24 hour prediction horizon.

## 2. ECONOMIC LINEAR OPTIMAL CONTROL

The objective of Economic Linear Optimal Control (ELOC) is to develop a linear controller that approximates the economic motives of a large horizon EMPC. For background information regarding the development of this methodology, the reader is encouraged to review Peng *et al.* (2005), Mendoza-Serrano and Chmielewski (2012b), and Omell and Chmielewski (2013 and 2014). For the sake of brevity, only the general aspects and results are presented in this work. As such, we begin by discussing the main differences between EMPC and ELOC. First, ELOC is such that inequality constraints are enforced statistically. This means that the control limits can be violated as long as each variable of interest remains within the probabilistic allowances given in the formulation. Additionally, ELOC incorporates the disturbance model as part of the formulation. This provides it with knowledge of the oscillating nature of the disturbance variables, which is essential for making control decisions. The result of

applying ELOC to the HVAC building example are given in Figure 5 (left), where the electricity price is assumed to have a variance  $\Sigma_{C_e} = (7.175 \text{ \$/MWhr})^2$  and  $\bar{C}_e = 24.8 \text{ \$/MWhr}$ . Clearly, the actions of the ELOC are similar to those of EMPC. It is additionally noted that the optimization problem used to determine the ELOC policy, while not convex is easily solved to its global optimum. This particular feature will be exploited when we return to the equipment sizing problem.

Of course, the ELOC policy cannot be implemented due to its inability to enforce point-wise-in-time constraints. Toward the enforcement of these point-wise-in-time constraints the linear feedback from the ELOC is converted to the form of a predictive controller by implementing inverse optimality (Chmielewski and Manthanwar, 2004). Once in predictive form, one can simply impose point-wise-in-time constraints to the predicted trajectories (Mendoza-Serrano and Chmielewski, 2012b; Mendoza-Serrano, 2013). Figure 5 (right) compares the Constrained ELOC trajectory with that of the EMPC and illustrates the enforcement of point-wise-in-time constraints. It is additionally noted that the plots of Figure 5 were made under the assumption of Zero Future Information (ZFI) with regard to disturbance measurements and relied heavily upon the disturbance model for disturbance forecasting. This is in contrast to the plots of Figures 3 and 4 that assumed Full Future Information (FFI) with regard to the disturbances. For details concerning disturbance models and the impact of forecasting methods, please see Mendoza-Serrano (2013) and Mendoza-Serrano and Chmielewski (2014). The primary advantage of the Constrained ELOC policy stems from its virtual insensitivity to horizon size. Table 1 illustrates that Constrained ELOC with a horizon of 2 yields a massive reduction in computational effort with only a minor sacrifice in economic performance as compared to the ZFI EMPC.

**Table 1:** Computational Efficiency of Constrained ELOC

	Computational Time (sec)	Computational Reduction (%)	Expenditure (\$/28days)	Expenditure Reduction (%)
EMPC FFI with No TES	-	-	759	-
EMPC FFI with N=24 hrs	13,321	-	521	31.4%
EMPC ZFI with N=24 hrs	-	-	556	26.7%
EMPC ZFI with N=2 hrs	6	99.95%	674	11.2%
Constrained ELOC ZFI N=2 hrs	4	99.97%	562	26.0%

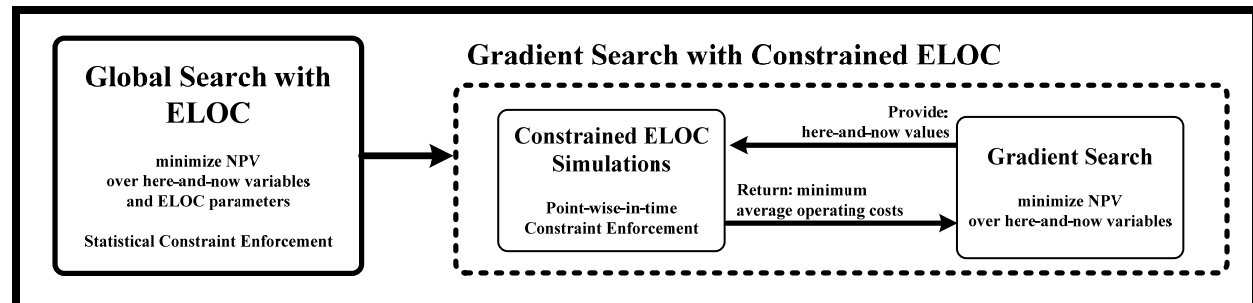


**Figure 6:** Proposed solution method for equipment sizing problem.

### 3. EQUIPMENT SIZING IMPLEMENTATION

Returning to the equipment sizing problem, the computationally burdensome EMPC policy can now be replaced by one of two possible surrogate policies – the ELOC and the Constrained ELOC. As we will see, the computational efficiency of each of these surrogates will enable a computationally tractable search over the equipment size variables. Figure 6 depicts the proposed procedure. The first step extends the ELOC optimization problem to one in which the ELOC policy and equipment size parameters are determined simultaneously. Then, this initial guess with regard to equipment size parameters is refined in the context of point-wise-in-time constraints using a gradient search based on the Constrained ELOC policy.

A central component of ELOC design problem is the constraint on the statistics of the process. In the HVAC problem these will manifest as the closed-loop standard deviation of power to the chiller must be less than one half of the maximum (or rated) power to the chiller:  $\sigma_P < P_c^{\max} / 2$ . Similarly, operation of the storage would have a constraint such as:  $\sigma_{E_S} < -E_S^{\min} / 2$ . It is then easily concluded that converting  $P_c^{\max}$  and  $E_S^{\min}$  from parameters to variables of the ELOC optimization problem will add virtually nothing to the computational complexity of the problem since each appears only linearly within the constraints. To complete the extension, the ELOC objective function will need to be replaced by one similar to Equation 5, where  $\bar{R}$  is the original ELOC objective function and the capital cost terms will need to be functions of  $P_c^{\max}$  and  $E_S^{\min}$ . In the current work, it is assumed that these functions are simple proportionality relations. In this case, computational complexity of the extended ELOC optimization will not be impacted. However, if the capital cost expressions are non-convex (which is expected to be the case in reality) then an efficient global search procedure will be required. One such approach can be found in Omell (2013).

To illustrate the ELOC based equipment sizing method assume the parameters of Equation 7 are  $r_i = 7\%$  and  $n = 30$  yrs. In addition, assume the capital costs are  $c_S E_S^{\min} + c_C P_c^{\max}$ , where  $c_C = \$500/kW_e$  and  $c_S = -\$28.4/kW_7hr$ . In this case, the ELOC based method determines that the optimal configuration is one without any TES, and as indicated in the left plot of Figure 7, selects an ELOC policy that runs the system as such. If the cost of storage is reduced to  $c_S = -\$14.2/kW_7hr$ , then it concludes that the optimal storage unit size is  $-604.7 kW_7hr$  and the chiller size can be reduced a bit to  $38.7 kW_e$ . The center plot of Figure 7 indicates the closed-loop behavior under the corresponding ELOC policy. If the cost of storage is drastically reduced to  $c_S = -\$2.8/kW_7hr$ , then the ELOC based search concludes that the storage unit should be used compensate for changes in outside temperature while the chiller is run virtually at steady-state. It should be noted that in all three cases the resulting ELOC policy does not attempt to use the TES to time shift energy purchases. For this to be the case, either the chiller capital costs would need to be much lower or the expected variability in electricity price would need to be much higher. See Mendoza-Serrano and Chmielewski (2012a) for additional details.

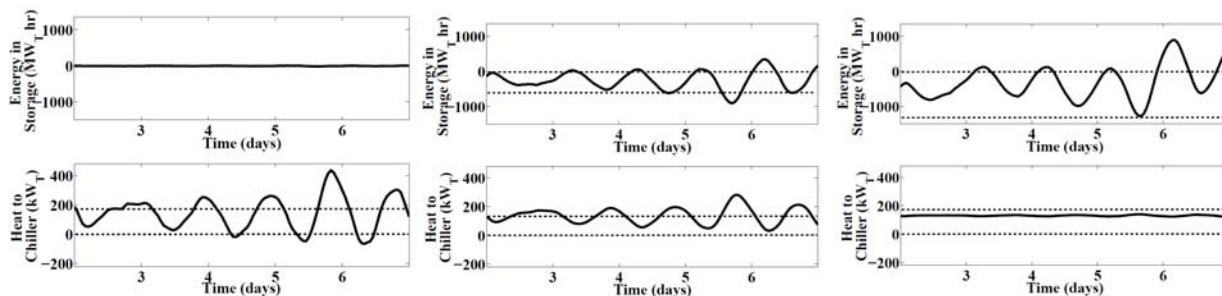


**Figure 7:** Closed-loop ELOC trajectories and equipment sizes resulting from the ELOC based search.  
Left –  $c_S = -\$28.4/kW_7hr$ . Center –  $c_S = -\$14.2/kW_7hr$ . Right –  $c_S = -\$2.8/kW_7hr$ .

From the plots of Figure 7 it is clear that the point-wise-in-time constraints are not being observed. Thus, the second step of the procedure of Figure 6 is to perform a gradient search based on the Constrained ELOC, which will enforce these point-wise-in-time constraints. Given the solution determined by the ELOC based search, this gradient search will have a reasonable starting point with regard to the equipment sizes as well as have the ELOC parameters required to construct the Constrained ELOC policy. Furthermore, due to the computational speed of the Constrained ELOC this gradient search will be computationally tractable. It should be emphasized that we make no claim of a global solution resulting from this gradient search. We do, however, note that global solution resulting from the ELOC based search (which is flawed in the sense that point-wise-in-time constraints are not enforced) increases the likelihood of having a starting point close to the true global solution.

As an illustration, consider the case of  $c_S = -\$14.2/kW_7hr$ , which provided a solution of  $E_S^{\min} = -604.7 kW_7hr$  and  $P_c^{\max} = 38.7 kW_e$ . Using the ELOC feedback of that solution the constrained ELOC was constructed, and as an aid to the reader the contour plot of Figure 8 (left) was constructed by calculating the NPV at each point of the search

space. Then using the equipment sizes determined from the ELOC based search as a starting point, the gradient search was implemented as illustrated in the right plot of Figure 8.

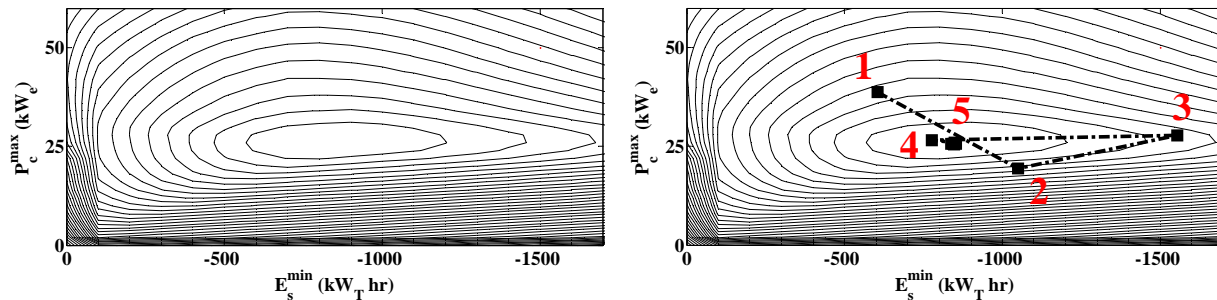


**Figure 8:** Illustration of the Constrained ELOC based gradient search

The one remaining computational issue concerns the proper evaluation of NPV when the postulated equipment sizes cannot meet the process constraints. In the HVAC context, the problem is most likely to occur when the chiller is under sized. In this case, there may be a set of weather conditions such that the cooling load is sufficiently large and the system is unable to satisfy the comfort constraints, specifically room temperature less than 25C. If this is the case, then that particular chiller size should be deemed infeasible. The difficulty stems from the fact that the boundary between feasibility and infeasibility can only be determined numerically and in the HVAC case will also be a function of postulated TES size. One way to look at this question of infeasibility is to set the NPV of such a point equal to infinity, which would bar that point from being a solution. However, in the context of a gradient search algorithm, such an approach will leave the algorithm at a loss for the next search point, since no gradient will exist at that point. An alternative is to reformulate the Constrained ELOC problem using soft constraints (Zheng and Morari, 1995). This will allow for violations of the comfort constraints, but only when the policy has no other alternative. Then, during the Constrained ELOC simulations, one could keep track of the size and duration of the constraint violations. In the results to follow we computed the integral of the violations to determine an area associated with the violations. Then, this area was multiplied by a penalization factor,  $p$ , and then added to the NPV calculated by the simulation.

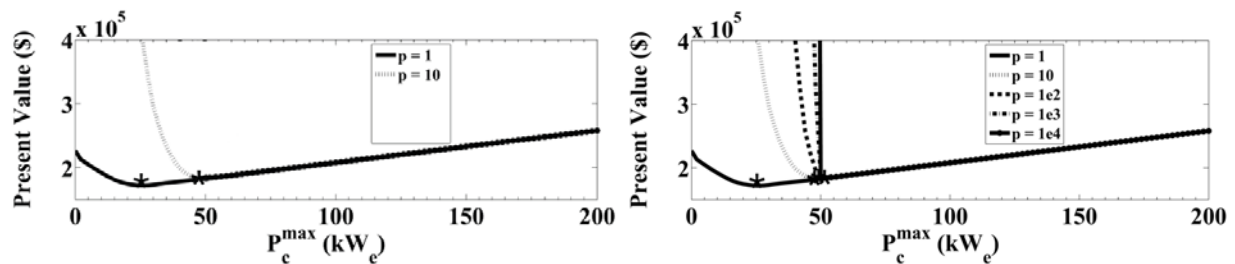


**Figure 9:** Cross sectional view of  $P_c^{max}$  with penalization factors.

**Table 2:** Equipment sizing gradient search trajectory

Penalty	$E_s^{min}$ (kW <sub>T</sub> hr)	$P_c^{max}$ (kW <sub>e</sub> )
	-604.7	38.7
1	-845.0	25.6
1e1	-1105.1	48.9
1e2	-1295.9	46.8
1e3	-1098.5	49.9
1e4	-1098.5	49.9

The plots of Figure 8 actually used this approach with a penalization factor  $p = 1$ . The left plot of Figure 9 shows a slice of the contour plot through the fifth point of Figure 8, indicated by the star at  $P_c^{max} = 25.6$  kW<sub>e</sub>. Then, the entire gradient search is repeated, using this point and the initial, but with  $p = 10$ . The result is a new solution at the point  $P_c^{max} = 48.9$  kW<sub>e</sub>. Further increases of the penalization factor are depicted in the right plot of Figure 9. Notice that for

large penalization factors the NPV quickly approaches infinity for  $P_c^{max}$  values smaller than 49.9  $kW_e$ . If one were to have started the gradient search with these large penalization factors, then the gradient search would certainly have found it difficult to converge. Table 2 indicates the progression of the gradient search iterations.

## REFERENCES

- Chen, H., Cong, T. N., Chunqing, T., Li, Y., Ding, Y., 2009, Progress in electrical energy storage system: A critical review, *Prog. Nat. Sci.*, vol. 19, p. 291-312.
- Chmielewski, D. J., Manthanwar, A. M., 2004, On the tuning of predictive controllers: Inverse optimality and the minimum variance covariance constrained control problem, *Ind. Eng. Chem. Res.*, vol. 43, p. 7807-7814.
- Ercot, 2012, Historic real time data electricity prices for Houston Texas, <http://www.ercot.com/mktinfo/prices/>, (accessed on November 30, 2012).
- Farhangi, H., 2010, The path of the smart grid, *IEEE Power and Energy Magazine*, vol. 8, no. 1: p.18-28.
- Henze, G. P., Krarti, M., Brandemuehl, M. J., 2003, Guidelines for improved performance of ice storage systems, *Energy and Buildings*, vol. 35, p. 111-127.
- Ipakchi, A., Albuyeh, F., 2009, Grid of the future. *IEEE Power and Energy Magazine*, vol. 7, no. 2: p. 52-62.
- Lima, R.M., Grossmann, I.E., Jiao, Y., 2011, Long-term scheduling of a single-unit multi-product continuous process to manufacture high performance glass, *Computers & Chemical Engineering*, vol. 35, p. 554–574.
- Mendoza-Serrano, D. I., 2013, *Smart grid coordination in building HVAC systems*, PhD Dissertation, IIT.
- Mendoza-Serrano, D. I., Chmielewski, D. J., 2012a, Controller and system design for HVAC with Thermal Energy Storage. *Proc. of the 51st IEEE Conference on Decision and Control*, Hawaii, USA.
- Mendoza-Serrano, D. I., Chmielewski, D. J., 2012b, HVAC control using infinite-horizon economic MPC. *Proc. of the Am. Contr. Conf.*, Montreal, CA.
- Mendoza-Serrano, D. I., Chmielewski, D. J., 2014, Smart grid coordination in building HVAC systems: EMPC and the impact of forecasting, *J. Proc. Contr.*, submitted.
- National Climatic Data Center (NCDC), 2012, Hourly climate data for Houston Texas: <http://www.ncdc.noaa.gov/oa/climate/climatedata.html>, (accessed on November 30, 2012).
- Omell, B. P., 2013, *Economic based control system design*, PhD Dissertation, IIT.
- Omell, B. P., Chmielewski, D. J. 2013, IGCC power plant dispatch using infinite-horizon economic model predictive control, *Ind. Eng. Chem. Res.* vol. 52, no. 9, p. 3151-3164.
- Omell, B.P., Chmielewski, D.J., 2014, On the tuning of predictive controllers: Impact of disturbances, constraints and feedback structure, *AIChE J.*, accepted.
- Peng, J. K., Manthanwar, A. M., Chmielewski, D. J., 2005, On the tuning of predictive controllers: The minimally backed-off operating point selection problem, *Ind. Eng. Chem. Res.*, vol. 44, p. 7814-7822.
- Walawalkar, R., Chevva, K. R., Fernands, S., Thakur, N., 2010, Evolution and current status of demand response (DR) in electricity markets: Insights from PJM and NYISO, *Energy*, vol. 35, no. 4: p. 1553-1560.
- Zheng, A., Morari, M., 1995, Stability of model predictive control with mixed constraints. *IEEE Tran Aut. Contr.*, vol. 40 no. 10, p. 1818-1823.

## ACKNOWLEDGEMENT

The authors would like to thank the National Science Foundation (CBET – 0967906) and the Wanger Institute for Sustainable Engineering Research at the Illinois Institute of Technology for financial support.